

Original Article

Juvenile Plasma Factors Improve Organ Function and Survival following Injury by Promoting Antioxidant Response

Xiaogang Chu¹, Kumar Subramani¹, Bobby Thomas², Alvin V. Terry, Jr¹, Sadanand Fulzele³, Raghavan Pillai Raju^{1,*}

¹Department of Pharmacology and Toxicology, Medical College of Georgia, Augusta, GA 30912, USA. ²Departments of Pediatrics, Neuroscience and Drug Discovery, Darby Children's Research Institute, Medical University of South Carolina, Charleston, SC 29425, USA. ³Department of Medicine, Medical College of Georgia, Augusta, GA 30912, USA.

[Received June 19, 2021; Revised August 27, 2021; Accepted August 30, 2021]

ABSTRACT: Studies have shown that factors in the blood of young organisms can rejuvenate the old ones. Studies using heterochronic parabiosis models further reinforced the hypothesis that juvenile factors can rejuvenate aged systems. We sought to determine the effect of juvenile plasma-derived factors on the outcome following hemorrhagic shock injury in aged mice. We discovered that pre-pubertal (young) mice subjected to hemorrhagic shock survived for a prolonged period, in the absence of fluid resuscitation, compared to mature or aged mice. To further understand the mechanism of maturational dependence of injury resolution, extracellular vesicles isolated from the plasma of young mice were administered to aged mice subjected to hemorrhagic shock. The extracellular vesicle treatment prolonged life in the aged mice. The treatment resulted in reduced oxidative stress in the liver and in the circulation, along with an enhanced expression of the nuclear factor erythroid factor 2-related factor 2 (Nrf2) and its target genes, and a reduction in the expression of the transcription factor BTB and CNC homology 1 (Bach1). We propose that plasma factors in the juvenile mice have a reparative effect in the aged mice in injury resolution by modulating the Nrf2/Bach1 axis in the antioxidant response pathway.

Key words: aging, exosomes, extracellular vesicles, shock, juvenile factors

Aging systems reduce agility of the organism and contribute to an increased propensity for injuries [1, 2]. Furthermore, the age-associated changes in the cellular response to injury impair recovery [3-6]. Our laboratory and others have demonstrated a declined organ function following hemorrhagic shock injury (HI) which is exacerbated with aging [2, 5-8]. Oxidative stress has been reported to be one of the critical pathological hallmarks of HI [9, 10]. The inter-relationship between oxidative stress and cellular energetics triggers a vicious cycle post-injury, as an excessive production of oxidants results in impaired

cellular functions leading to organ dysfunction and mortality. The transcription factor nuclear factor erythroid 2-related factor 2 (Nrf2) is a "master regulator" of the antioxidant responses and plays a key role in maintaining redox homeostasis [11]. Nrf2 modulates the expression of hundreds of genes, that regulate antioxidants, cytoprotection, anti-inflammatory processes, tissue remodeling and fibrosis, carcinogenesis and metastasis [12, 13]. Thus, the dysregulation of the Nrf2 signaling network of critical gene products is a likely cause for the

*Correspondence should be addressed to: Dr. Raghavan Pillai Raju, Department of Pharmacology and Toxicology, Medical College of Georgia, Augusta, GA 30912, USA. Email: RRaju@augusta.edu.

Copyright: © 2021 Chu X et al. This is an open-access article distributed under the terms of the [Creative Commons Attribution License](https://creativecommons.org/licenses/by/4.0/), which permits unrestricted use, distribution, and reproduction in any medium, provided the original author and source are credited.

perpetuation of oxidative stress resulting in the disease pathology.

While exogenous agents that modulate injury response pathways are being extensively investigated, very little is known about endogenous factors that can restore homeostasis following injury. Transfer of young blood to old animals by heterochronic parabiosis is known to have protective effects in injury as well as in organismal aging [14-16]. However, the identity or the mechanism of maturation-dependent factors in the blood that have reparative effects remain to be determined. Studies have demonstrated that transfer of blood from young animals to aged ones reduced infarct size in stroke [17], reversed age-related cardiac hypertrophy [18], and rejuvenated aged progenitor cells [19]. Stem cells and stem-cell derived extracellular vesicles (EVs) were investigated in several laboratories as therapeutic agents for different disease conditions [20-22]. The EVs derived from bodily fluids, including blood plasma, have been effectively used in experimental models of human diseases [23, 24]. In this study, we hypothesized that juvenile plasma-derived EVs can potentiate metabolic networks converging on cellular energetics, attenuate oxidative stress, and improve outcomes following injury in the aged mice. We tested this hypothesis by treating aged mice subjected to HI with EVs isolated from young mice (Y-EVs).

MATERIALS AND METHODS

Animals

Young (5–6-week-old) and mature (3–4-month-old) male C57BL/6 mice used were obtained from Jackson laboratories and aged (23–26-month-old) C57BL/6 mice were from the National Institute of Aging rodent colony. Animal studies were conducted as per the protocol approved by the Institutional Animal Use and Care committee at the Augusta University. Hemorrhagic shock was induced as described before [25]. Briefly 60% blood volume was removed in 45 minutes through femoral artery, to induce hypovolemic shock (Mean arterial pressure: 30-35 mm Hg) and this MAP was maintained for another 45 minutes (shock period). Sham animals were not subjected to bleeding or fluid resuscitation, but they were subjected to laparotomy and groin incisions. For survival studies, EVs or vehicle was given immediately after the shock period (Fig. 1A). Each group for this study had 5-6 animals. For organ function studies, the animals were resuscitated following shock period for 1 hour, with Ringers Lactate (twice the shed blood volume), observed for another two hours and sacrificed to remove tissues for mitochondrial function assessment (Fig. 2A). Each group for this study had 6 animals. In this

latter group, EVs or vehicle was administered as a single dose (50 μ l; 2 mg/Kg body weight) at 10 minutes after the start of fluid resuscitation.

Preparation of EVs

The plasma EVs-enriched fractions were prepared as follows and as described in Ref. [26]. Briefly, plasma was diluted into 500 μ L PBS followed by centrifugation at 3000 RPM for 20 min to remove cell debris. The supernatant was collected and again centrifuged at 8000 RPM for 30 min to remove the remaining cell debris (1-3). The supernatant was collected and then Total Exosome Isolation Reagent (Life Technologies, Carlsbad, CA, USA) was used to isolate EVs as per manufacturer protocol. This protocol involved initial precipitation followed by centrifugation. After centrifugation, pellets were dissolved in phosphate-buffered saline (PBS) as EVs enriched fractions. EV concentrations were normalized by total protein level.

Mitochondrial respiration

The Seahorse XFp Analyzer (Seahorse Biosciences, North Billerica, MA) was used according to the manufacturer's protocol to measure oxygen consumption rate (OCR). Splenocytes or MEF cells were plated in XFp base medium, minimal DMEM (Seahorse Biosciences, North Billerica, MA) supplemented with 1mM pyruvate, 2mM glutamine, 10mM glucose (Sigma) at a density of 3×10^5 cells per well in specialized XFp miniplates pretreated with Cell Tak (Fisher). Plates were spun for 1 minute at 200 x g to ensure cell adhesion, and then incubated for 30 minutes at 37 °C prior to loading into the Seahorse analyzer. The following mitochondrial inhibitors were sequentially injected: oligomycin (1 μ M), carbonyl cyanide p-(trifluoromethoxy) phenylhydrazone (FCCP) (0.3 μ M), antimycin A and rotenone (1 μ M) and OCR measured. OCR values of the cells from animals in HI group were normalized to that of the sham-operated animals. Samples from 6 sham animals and 4 animals each in each HI and treatment groups were used.

Liver mitochondria: Mice liver mitochondria were extracted using tissue mitochondria isolation kit (#k288-50, BioVision, Milpitas, CA). Samples were from 4 sham animals and 3 animals each in each HI and treatment groups. Isolated liver mitochondria were diluted to 4 μ g/25 μ l in cold MAS buffer + substrate (pyruvate/malate) and plated onto 8-well XFp plates for OCR measurements. The plate was centrifuged at 2000g for 20 min at 4°C to attach the mitochondria. After centrifugation, an additional 155 μ l of MAS buffer + substrate was added to the wells. Mitochondria were checked under the microscope to ensure a homogeneous

mitochondrial monolayer in each well and incubated at 37°C for 10 min. The plates were further equilibrated for 8 min before the measurement of basal respiration. The final concentrations of compounds after injections were as follows: 4 mM ADP, 3 μM oligomycin, 4 μM FCCP, and 4 μM antimycin A. Respiratory state was calculated by the Seahorse XF software package

JC-1 assay for mitochondrial membrane potential

The experiment was performed using Isolated Mitochondria Staining kit (Sigma Chemical Co., St. Louis, MO). Samples from 4 animals were used in each group. Briefly, 5 μg sample of isolated mitochondria (BioVision, Milpitas, CA) was stained with a 0.2 μg/mL JC-1 solution. For a control, valinomycin, an ionophore, was added to an identical 5 μg sample of isolated mitochondria to a final concentration of 0.5 μg/mL. Four animals were used in each group. This sample was placed on ice for 10 minutes to allow complete dissipation of the membrane potential, and then stained with a 0.2 μg/mL JC-1 solution and assayed in parallel. Samples were read over a period of 30 minutes using a BIOTEK (Synergy HT) fluorescence plate reader (excitation wavelength = 485 nm, emission wavelength = 590 nm). Results are expressed as a percentage of the valinomycin baseline control fluorescence.

Cell Culture

WT and NRF2^{-/-} MEF cells were maintained as sub confluent monolayers in Dulbecco's Modified Eagle's medium (Gibco, Waltham, MA) supplemented with 10% fetal bovine serum (HyClone, Logan, UT) and 100 units/ml penicillin plus 100 μg/ml streptomycin (Invitrogen, Waltham, MA) at 37°C in 5% CO₂. Cells were treated with 100 μg/ml EVs or media for the durations indicated.

Immunoblotting Analysis

Immunoblotting procedures were performed as we described previously [25]. Briefly, tissues or cells were homogenized in the lysis buffer. Lysates were clarified at 12,000 g for 10 min at 4°C, and protein concentrations were determined by the Bradford protein assay (Bio-Rad Laboratories, Hercules, CA). Equal amounts of protein were loaded onto 8–12% SDS-PAGE, transferred onto polyvinylidene difluoride membranes, probed with the indicated primary antibody and the appropriate secondary antibody conjugated with horseradish peroxidase (Cell Signaling, Danvers, MA), and the immune complexes were detected by standard methods. Samples from 5-6 animals were used for this study. 2-3 technical replicates

were used in each experiment. 6 replicates were used for *in vitro* experiments except for Figure 8B where 4 replicates were used. The antibodies used in this study are listed in Supplementary Table 1.

Real-Time Polymerase Chain Reaction

Total RNA was isolated using TRIZOL reagent (Thermo Fisher Scientific, Waltham, MA) and cDNA was synthesized using ImProm-II™ Reverse Transcription System (Promega, Madison, WI). Realtime PCR was performed using standard protocols. Samples from 5-6 animals were used for PCR analysis. 2-3 technical replicates in each experiment. 6-9 replicates were used for *in vitro* experiments. The sequences of the primers used in this study are listed in Supplementary Table 2.

Lactate assay

The plasma was separated by centrifugation (2,000 g, 10 min) and stored at -80 °C until assayed for lactate levels. Samples from 5-6 animals were used. Lactate levels were measured using a Lactate Assay Kit (Sigma, St. Louis, MO) according to the manufacturer's protocol.

MDA and H₂O₂ assay

Plasma malondialdehyde (MDA) was determined using the TBARS (Thiobarbituric Acid Reactive Substances Assay) Kit (Cayman Chemical, Ann Arbor, MI) according to the manufacturer's protocol. Samples from 5 animals/group were used. H₂O₂ assay was carried out using the Amplex Red Assay from Invitrogen (ThermoFisher, MA) as per the manufacturer protocols.

NRF2 transcription factor assay

Mice liver nuclei were extracted using tissue nuclear extraction kit (Active motif, Carlsbad, CA) according to the manufacturer's protocol. Samples from 5 animals/group were used. Nrf2 transcription factor DNA binding activity were detected using Nrf2 transcriptional factor assay kit (#600590, Cayman Chemical, Ann Arbor, Michigan).

Statistics

Survival analysis was performed by Kaplan-Meier plot and significance between survival curves was determined using Graphpad Prism 9 (GraphPad Software, San Diego, CA). All statistical analysis were done using Graphpad Prism software. Data normality was tested by Shapiro-Wilk normality test. One-way ANOVA with Tukey's post hoc correction was used for normal data. Studies with

more than one independent variable were analyzed by two-way ANOVA with post hoc correction. Non-parametric test was done for data that did not pass the normality test. Two group comparisons were done by Mann-Whitney t-test.

RESULTS

The severe blood loss resulting in decompensated hemorrhagic shock is fatal unless the animals receive prompt fluid resuscitation or agents that can prolong life. These animals do not survive more than an hour following the shock period without intervention [25]. In this study, when mature or aged mice were subjected to HI and were

not resuscitated with fluid, the mean duration of survival observed was 30 and 34 minutes respectively (Fig. 1A-B), and the survival durations were not significantly different. However, when pre-pubertal (young) mice were subjected to hemorrhagic shock, in the absence of fluid resuscitation, these animals survived for a significantly prolonged period of time (mean=139 minutes) compared to mature or aged animals (Fig. 1-B). The results showed that young mice were more resilient than mature or aged mice to the severe whole-body insult of hemorrhagic shock. This experiment led us to test whether plasma factors in young mice could prolong survival in the aged mice following HI.

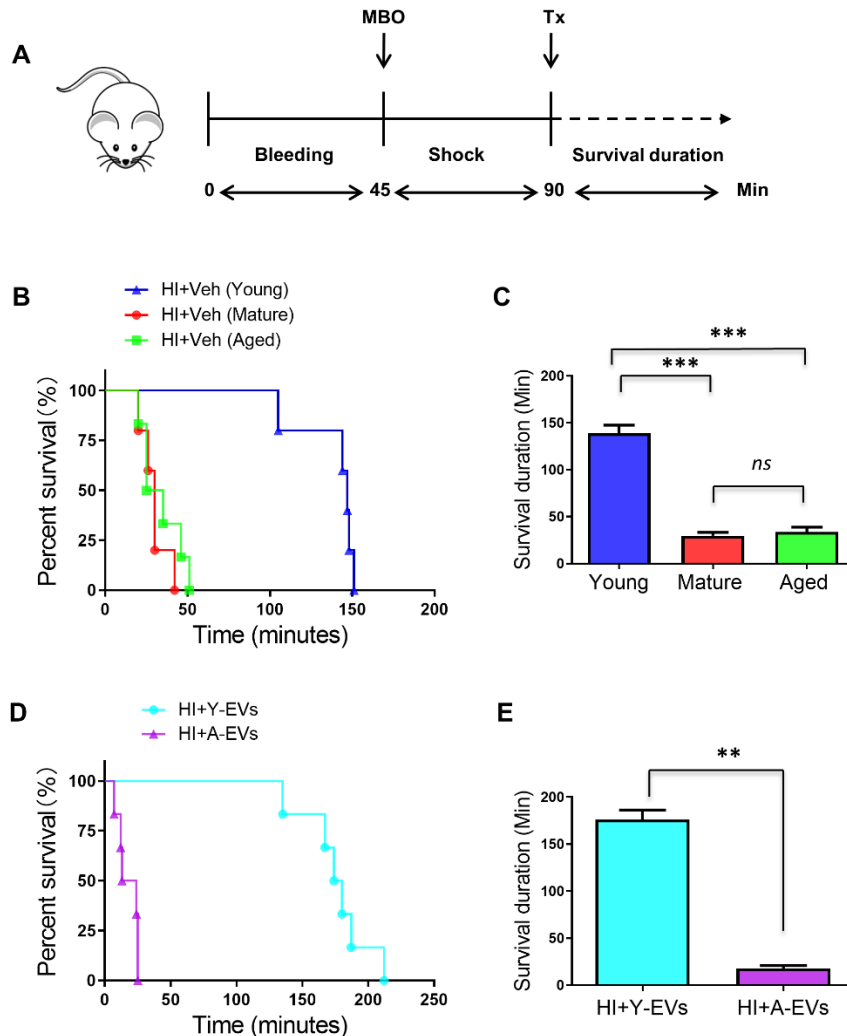


Figure 1. Effect of juvenile plasma factors on survival following HI. (A) Schematic representation of the experimental design for the hemorrhagic shock injury (HI): model for survival studies (no fluid resuscitation). MBO=maximum bleed out. Tx = treatment with Veh or EVs. (B) Kaplan-Meier survival curves for young, mature and aged mice subjected to HI. **indicates p<0.01; Veh=vehicle (C) Bar diagram represents mean duration of survival of the animals represented in panel B; mean ± SEM; ***indicates p<0.001. Survival duration is time from treatment (Tx). (D) Kaplan-Meier survival curves for aged mice subjected to HI. Y-EVs or A-EVs were administered after the shock period. EVs were isolated from the plasma of young (Y-EVs) or aged (Y-EVs) mice. (E) Bar diagram represents mean duration of survival of the animals represented in panel D; mean ± SEM; **indicates p<0.01. Survival duration is time from treatment (Tx).

We isolated extracellular vesicles (EVs) from the plasma of young mice (Y-EVs) and intravenously administered them to aged mice after HI, without resuscitating the mice with fluid. The aged animals that received Y-EVs survived for 176 minutes (mean value), compared to vehicle (veh)-treated mice that survived for 34 minutes (Fig. 1B-E). To test whether the improved survival was due to non-specific effect of EVs, another group of aged mice were treated with EVs isolated from aged mice. The aged mice that received EVs from the matching age group (A-EVs) showed a survival rate

comparable to the animals that did not receive EVs (Fig. 1D-E) demonstrating that EVs in the plasma of young mice, but not the EVs in the plasma of aged mice, have the reparative capacity in terms of prolonging survival after HI. Y-EVs also improved the mean arterial pressure (MAP) of aged mice following the HI procedure (Fig. 2A-B). As shown in Figure 2C, plasma lactate, an indicator of hypoxemia and OXPHOS-glycolytic switch, was significantly increased in animals subjected to HI compared to sham operated animals, but was restored in animals that received Y-EVs after HI.

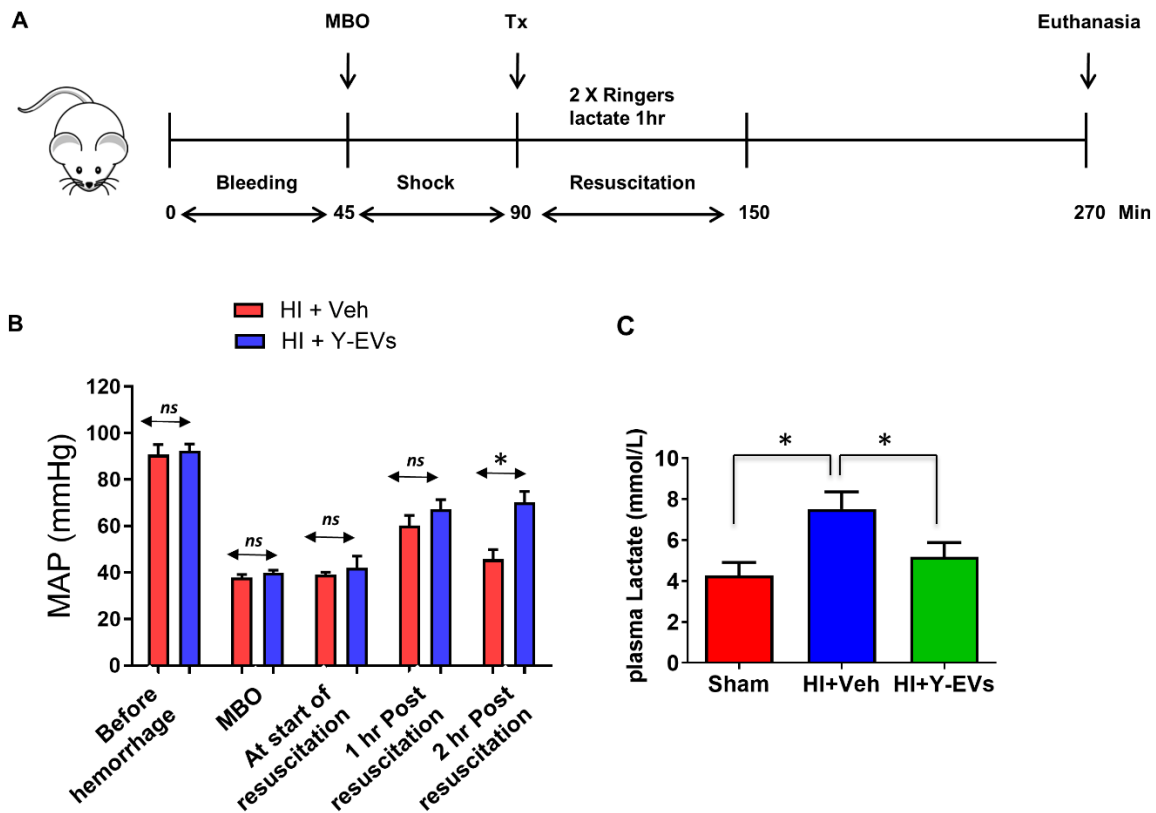


Figure 2. MAP and plasma lactate improved with Y-EVs treatment following HI. (A) Schematic representation of the experimental design for HI: model for organ function studies (with fluid resuscitation). (B) Mean arterial pressure (MAP) following HI and treatment with Y-EVs measured before hemorrhage, at maximum bleed out (MBO), at start of resuscitation, and at 1 and 2 h post resuscitation. mean ± SEM. *p < 0.05; ns = not statistically significant. Two-way ANOVA and Tukey’s multiple comparisons post hoc tests were used. (C) Plasma lactate levels. Groups: Sham, HI+Veh and HI+Y-EVs; mean ± SEM, *indicates p<0.05.

Next, considering the significance of cellular energetics in organ function maintenance, we tested whether Y-EVs treatment had any effect on mitochondrial respiration in the mice after HI. We isolated splenocytes from mice in experimental and control groups and evaluated mitochondrial respiration using a Seahorse analyzer. While the mito-stress test showed a significant decrease in the oxygen consumption rate (OCR) in aged mice following HI, Y-EVs treatment restored the OCR in

the splenocytes (Fig. 3A-E). The declined basal respiration, spare respiratory capacity, ATP production, as well as maximal respiration after HI were restored in Y-EVs-treated aged mice (Fig. 3B-E). In order to test whether a similar effect on mitochondrial function was present in other tissues, we isolated mitochondria from the liver of aged sham mice, mice subjected to HI and mice subjected to HI, but treated with Y-EVs. The liver is a critical organ affected in hemorrhagic shock [27]. HI

significantly decreased state III respiration and Y-EVs treatment attenuated the decrease (Fig. 3F). Consistent with these results, using mitochondria isolated from the liver, we observed that Y-EVs improved mitochondria membrane potential following HI (Fig. 3G). The declined mitochondrial function observed in various tissue

compartments following HI is consistent with previous reports from our laboratory and others demonstrating mitochondrial dysfunction following HI [28] [29] [30]. However, the improvement in mitochondrial respiration following the Y-EVs treatment demonstrates the effect of Y-EVs in maintaining cellular homeostasis following HI.

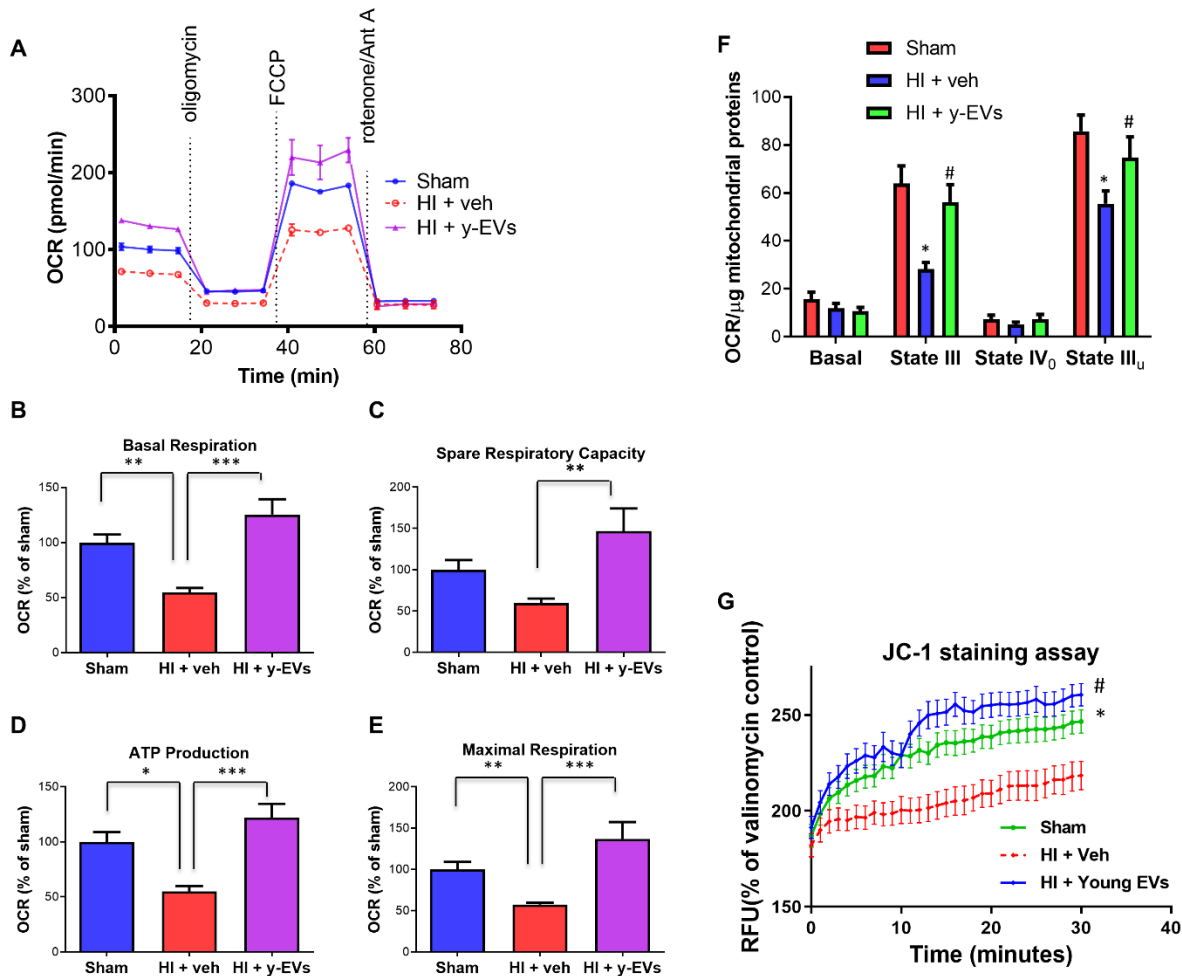


Figure 3. Mitochondrial function improved with Y-EVs treatment following HI. (A-E) Mitostress test on splenocytes. Splenocytes were isolated from aged mice in the following groups: sham, HI+Veh and HI+Y-EVs. Mitostress test was performed by sequential addition of oligomycin (complex V inhibitor), FCCP (mitochondrial membrane depolarization), rotenone (complex I inhibitor) and antimycin (Anti A- complex III inhibitor) in Seahorse analyzer. *= p<0.05, **=p<0.01 and ***=p<0.001. (F) Liver mitochondrial function assessment. Respiration of isolated mitochondria was measured using Seahorse analyser as described in Methods section. Groups: Sham, HI+Veh and HI+Y-EVs. *= p<0.05 compared to sham, # = p<0.05 compared to HI+Veh. (G) Liver mitochondrial permeability. Mitochondria were isolated from mouse liver as described in Methods section. Groups: Sham, HI+Veh and HI+Y-EVs. *= p<0.05 compared to sham at time=30mins # = p<0.05 compared to HI+Veh at time=30 mins (Two-way ANOVA and Tukey’s multiple comparisons post hoc tests were used). RFU – Relative Fluorescence units.

Next, we checked the gene and protein expression of molecular mediators of injury in the liver by real-time PCR and Western blot. As shown in Figure 4A, the mRNA expression of inflammatory cytokine genes IL1β and TNFα was significantly elevated in the liver of mice

subjected to HI, and the increase was attenuated in Y-EVs treated mice compared to the mice in Veh treated group. Consistent with the reduction of inflammatory and injury markers in Y-EVs treatment, phosphorylated JNK, phosphorylated eIF2α, as well as NLRP3 levels were

reduced while the level of phosphorylated P38 in Y-EVs treated animals was increased as compared to the controls indicating injury resolution following Y-EVs treatment (Fig. 4B-C). The results indicate significant reduction in

cell stress (p-JNK and Eif2a) and inflammation (NLRP3) following injury in animals treated with Y-EVs, thus demonstrating a therapeutic effect.

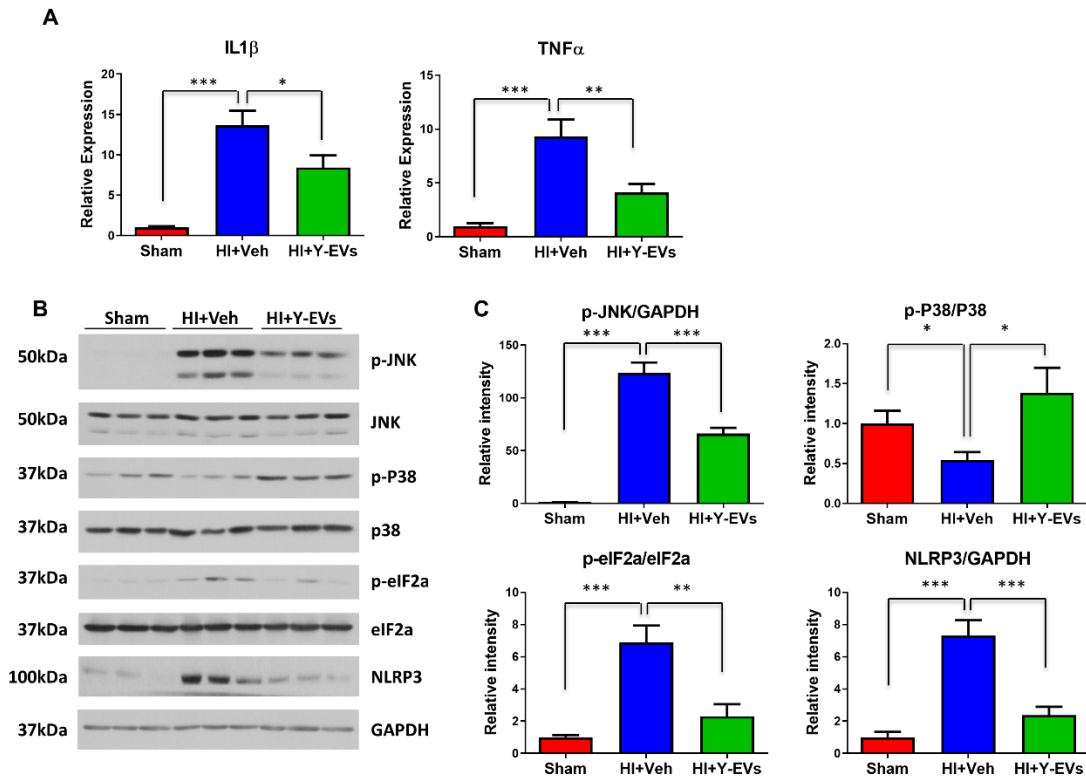


Figure 4. Effect of Y-EVs on liver inflammation following HI. (A) SYBR green real-time PCR amplification of IL1β and TNFα from the liver tissues. Groups: sham, HI+Veh and HI+Y-EVs; mean ± SEM; * = p<0.05, ** = p<0.01 and *** = p<0.001. (B) Representative Immunoblotting of p-JNK, JNK, p-P38, P38, p-eIF2a, eIF2a and NLRP3 using liver tissues. Groups: sham, HI+Veh and HI+Y-EVs. GAPDH was used as the loading control. The blots shown are representative of the replicates. (C) p-JNK/GAPDH, p-P38/P38, p-eIF2a/eIF2a and NLRP3/GAPDH ratios were quantified using Image J software (NIH), * = p<0.05, ** = p<0.01 and *** = p<0.001.

EVs regulate the activity of multiple physiological pathways, including the oxidative stress response, which is a hallmark of HI [31, 32]. We tested MDA and hydrogen peroxide (H₂O₂), two important oxidative stress markers in mice plasma. The concentration of both plasma MDA and H₂O₂ was significantly elevated in HI+veh group, and Y-EVs treatment effectively attenuated the increase (Fig. 5A-B). So, we next examined the expression changes in oxidative stress-related genes in the liver in the three groups of animals. However, as shown in Figure 5D, the expression of NQO1 and GPX2 in the liver were significantly decreased in mice subjected to HI, and restored in mice treated with Y-EVs, when compared to the Veh treated group. As both NQO1 and GPX2 are Nrf2-dependent antioxidant response genes, to explore the role of Y-EVs in Nrf2 signaling pathways, mice liver nuclear proteins were isolated and tested for the Nrf2 transcriptional activity. The change in expression level observed for the DNA-binding Nrf2 (Fig. 5C) followed

the same trend as NQO1 and GPX2. However, Hif1α and Bach1 gene expression was significantly elevated following HI and Y-EVs treatment attenuated the increase (Fig. 5D). Furthermore, though the expression level of Sod1 showed no difference between the sham and HI+veh group, Sod1 was significantly increased with Y-EVs treatment further indicating an elevated antioxidant response with Y-EVs (Fig. 5D). The expression changes in the genes for NQO1, HMOX1, GPX2 and NRF2 were also observed in the heart tissue (Supplementary Fig. 1). We also found that, consistent with increased Nrf2 activity upon Y-EVs treatment, Y-EVs increased the level of phospho-AKT, an upstream mediator of Nrf2 signaling (Fig. 5E). This data suggests that the failing Nrf2 response following HI is related to elevated levels of Bach1 and that this could be a reason for the lack of significant upregulation of the antioxidant response genes, NQO1 and GPX2.

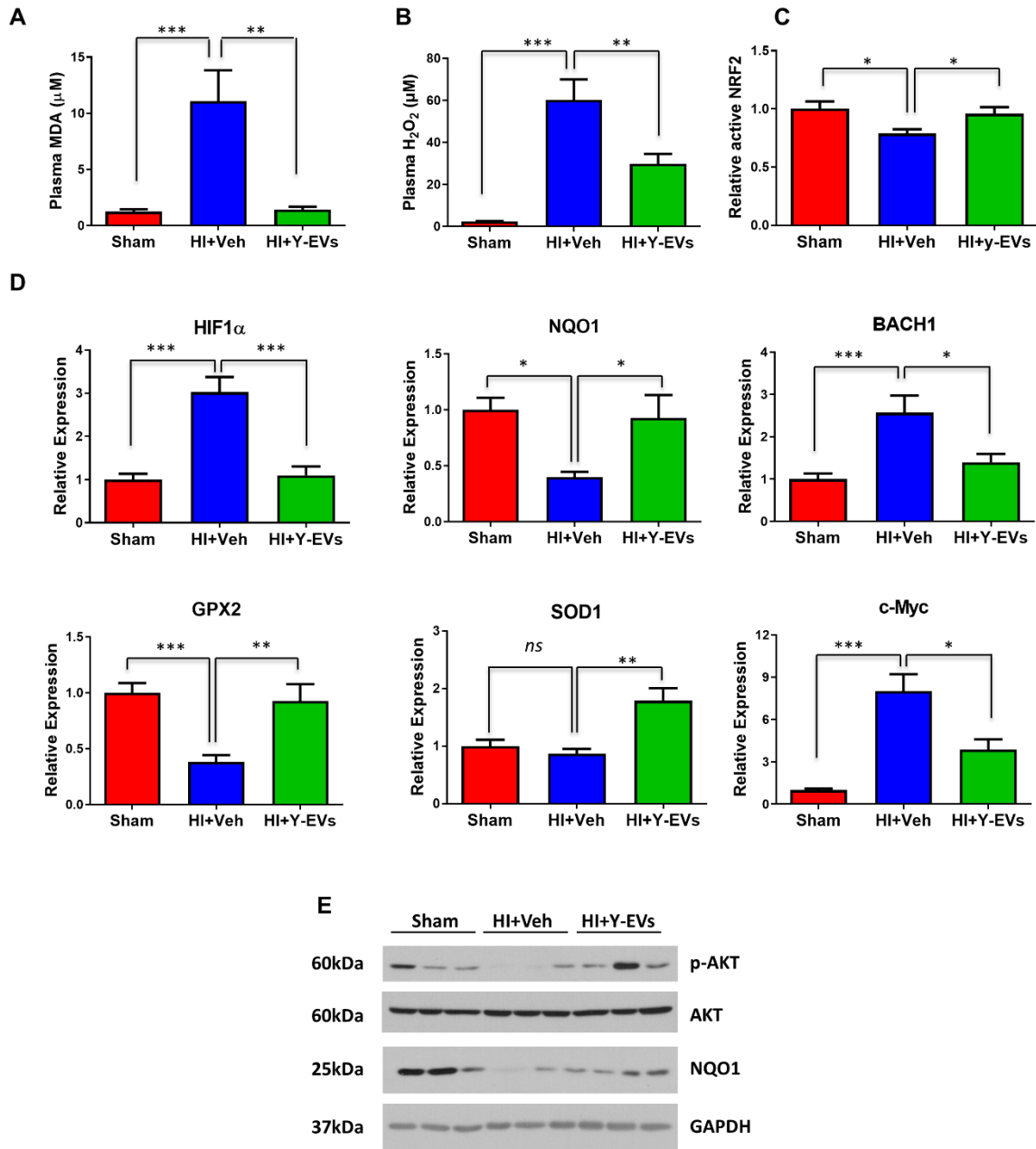


Figure 5. Y-EVs treatment on oxidative stress and antioxidant response following HI. (A-B) MDA and H₂O₂ concentrations in the plasma. The results shown represent mean ± SEM. ** =p<0.01 and *** =p<0.001. (C) Nrf2 transcriptional activity in liver. Mice liver nuclear fraction was tested for Nrf2 specific transcription factor DNA binding activity as described in the Methods section. The results shown represent mean ± SEM. * indicates p<0.05. (D) SYBR green real-time PCR amplification of NQO1, HIF1-α, GPX2, BACH1, SOD1 and c-Myc from the liver tissue. Groups: sham, HI+Veh and HI+Y-EVs. The results shown represent mean ± SEM. * =p<0.05, ** =p<0.01 and *** =p<0.001. (E) Representative Immunoblotting p-AKT, AKT and NQO1 in sham, HI+Veh and HI+Y-EVs. GAPDH was used as the loading control.

To understand the mechanisms underlying the effect of Y-EVs on HI associated oxidative stress, mouse embryonic fibroblast (MEF) cells were subjected to H₂O₂-induced oxidative stress in an *in vitro* model and mitochondrial respiration was measured using the Seahorse extracellular flux (XF) analyzer. In this

technique the mitochondrial oxygen consumption rate (OCR) is determined to measure oxidative phosphorylation (OXPHOS). H₂O₂ induced a decreased OCR demonstrating efficient reduction of mitochondrial respiration compared to the control (Fig. 6). This demonstrates significant impairment of the energetics

process driven by H₂O₂-induced oxidative stress. However, Y-EVs restored OCR thereby rescuing (Fig. 6A-E) MEF cells from the severe oxidative stress induced by exposure to H₂O₂. To further confirm H₂O₂-induced oxidative stress, the cells were treated with veh, Y-EVs or A-EVs following H₂O₂ treatment, then stained with CellRox green. As shown in Figure 6F-G, H₂O₂ exposure

significantly upregulated ROS production and Y-EVs treatment effectively attenuated the upregulation of ROS generation in response to H₂O₂. The oxidative stress induced in the presence of A-EVs was significantly higher than that observed in the presence of Y-EVs further demonstrating the antioxidant effect of Y-EVs.

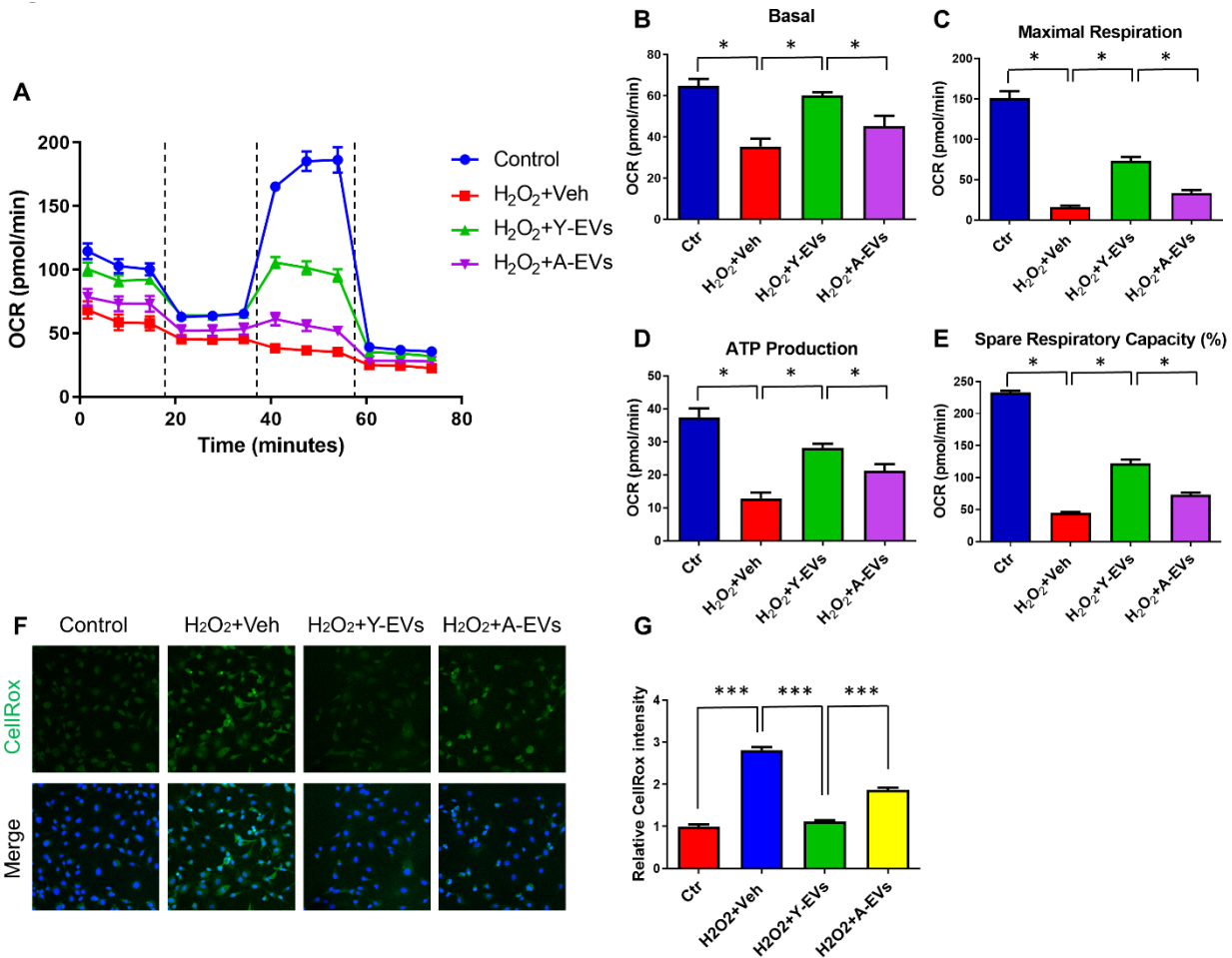


Figure 6. Effect of Y-EVs on mitochondrial function and oxidative stress induced in MEF cells. (A) Mitostress test with Y-EVs treated MEF cells following oxidative stress. MEF cells were treated with 200μM H₂O₂ and incubated with vehicle Y-EVs or A-EVs for 3 hours. Representative experiment. Mitostress test was performed by sequential addition of oligomycin (complex V inhibitor), FCCP (mitochondrial membrane depolarization), rotenone (complex I inhibitor) and antimycin (Anti A-complex III inhibitor). (B-E) Basal respiration, maximal respiration, ATP production, and spare respiration capacity were calculated from the data in panel A; * indicates p<0.05. (F) MEF cells were treated with 200μM H₂O₂, followed by vehicle, 100 μg/ml young EVs or aged EVs for 3 hours, then incubated with 5 μM CellROX® green reagent under culture conditions for 30 min and fixed with 4% PFA. Cells were stained with Hoechst for DNA. (G) CellROX green intensity was quantified using Image J software (NIH), *** indicates p < 0.001. At least 25 cells were measured in each group.

Next, we tested whether Y-EVs treatment could lead to modulation of Nrf2 signaling in H₂O₂ -induced oxidative stress *in vitro*, MEF cells were treated with vehicle, Y-EVs or A-EVs following H₂O₂ stress. The premise was based on our *in vivo* experiments that showed that intravenous administration of Y-EVs following HI

led to the activation of Nrf2 signaling pathways and inhibition of oxidative stress in the mouse liver. The gene and protein expression of Nrf2 associated molecular mediators was tested as shown in Figure 7A, H₂O₂ treatment resulted in a significant increase in the expression of genes for Hmox1, NQO1, Nrf2 and Bach1.

The data show an oxidative stress-driven antioxidant response with the H₂O₂ exposure. Whereas, Y-EVs treatment further increased the expression of Hmox1 and NQO1, Bach1 expression was reduced compared to that in veh or A-EVs treated cells. It was noteworthy that the treatment with veh, Y-EVs or A-EVs did not alter Nrf2 gene expression (Fig. 7A). As oxidative stress induces proinflammatory cytokine responses, we also checked the expression level of IL6, IL2 and IL1β. As shown in Figure 7A, H₂O₂ treatment promoted the expression of IL6, IL2

and IL1β, but treatment with Y-EVs significantly attenuated the expression of IL6 and IL1β, but not IL2, compared to veh treatment. Interestingly, A-EVs treatment further augmented the expression of IL6 and IL2 compared to that in Y-EVs treated cells (Fig. 7A). Whereas the in vitro experiments further demonstrate that Y-EVs reduce oxidative stress, our results also show that A-EVs cargo may contain factors that promote inflammation (Fig. 7).

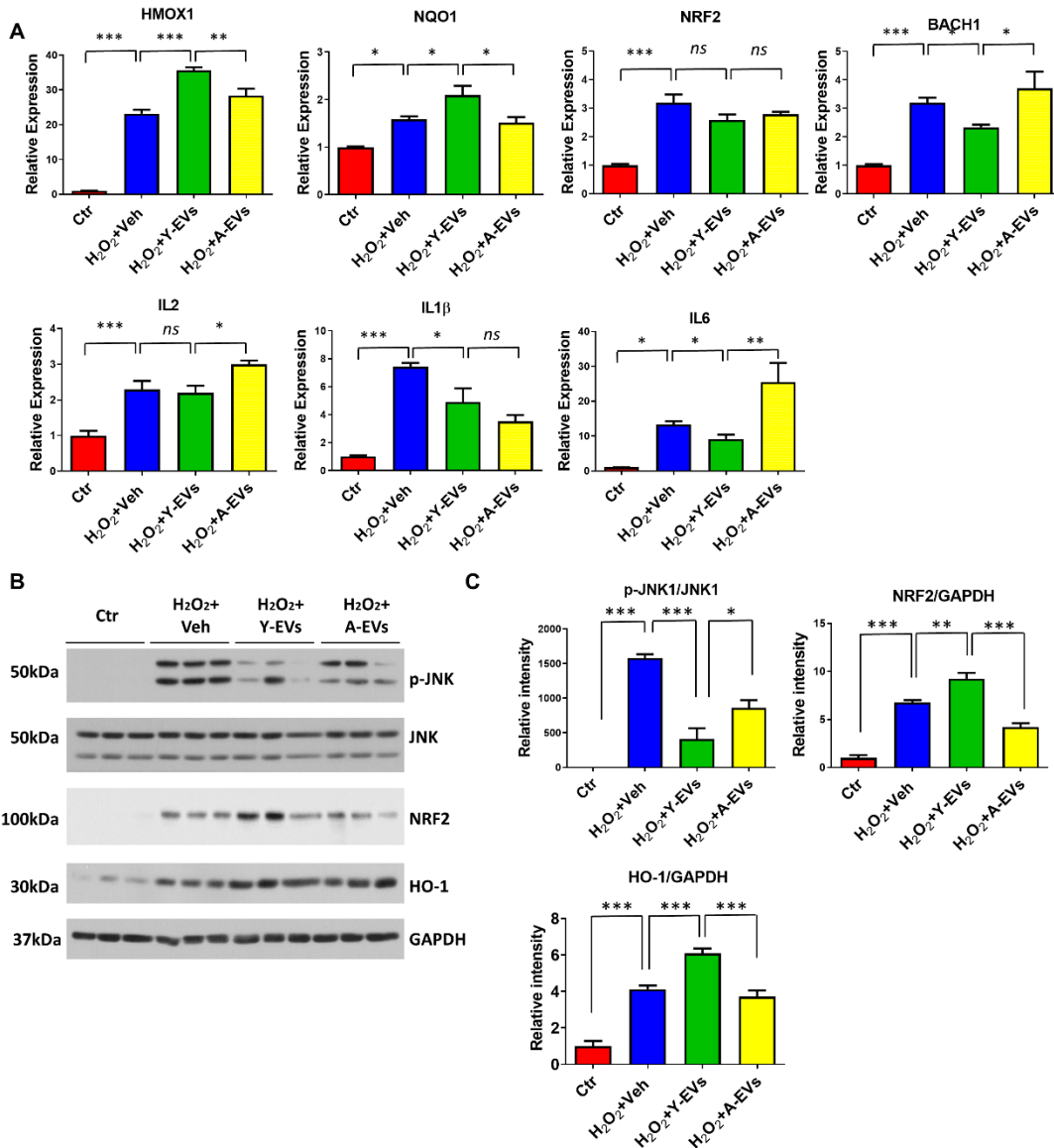


Figure 7. Effect of Y-EVs on oxidative stress and inflammation in MEF cells. (A) SYBR green real-time PCR amplification of HMOX1, NQO1, NRF2, BACH1, IL6, IL2 and IL1β. MEF cells were treated with 200μM H₂O₂, and added vehicle, Y-EVs or A-EVs for 3 hours. The results shown represent mean ± SEM. * indicates p<0.05; ns = not statistically significant. (B) Representative immunoblotting of p-JNK, JNK, NRF2 and HO-1 in control, H₂O₂+Veh, H₂O₂+Y-EVs and H₂O₂+A-EVs. MEF cells were treated with 200μM H₂O₂ and incubated with vehicle, Y-EVs or A-EVs for 3 hours. GAPDH was used as the loading control. (C) p-JNK/JNK, NRF2/GAPDH and HO-1/GAPDH ratios were quantified using Image J software (NIH), * indicates p < 0.05.

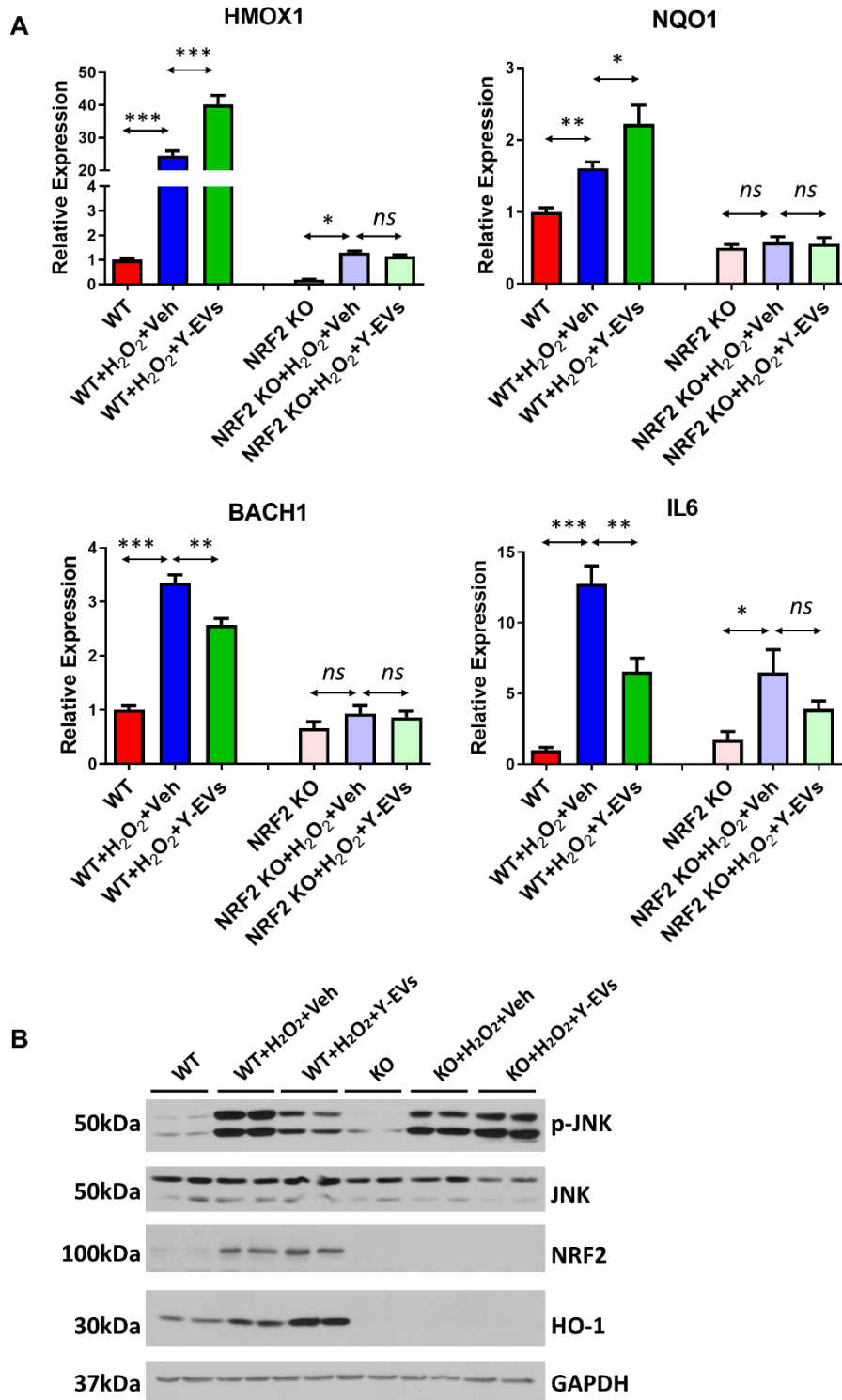


Figure 8. Effect of Y-EVs on MEF cells is Nrf2 dependent. (A) WT and NRF2 knock-out (KO) MEF cells were treated with 200μM H₂O₂, followed by vehicle or Y-EVs for 3 hours. SYBR green real-time PCR amplification of HMOX1, NQO1, BACH1 and IL6. The results shown represent mean ± SEM. * indicates p<0.05; ns = not statistically significant. (B) Representative Immunoblotting of p-JNK, JNK, NRF2 and HO-1 in control, H₂O₂+Veh, H₂O₂+Y-EVs and H₂O₂+A-EVs. WT and NRF2 knock-out MEF cells were treated with 200 μM H₂O₂, followed by vehicle, Y-EVs or A-EVs for 3 hours. GAPDH was used as the loading control. The blots shown are representative of the replicates.

To further determine the role of Y-EVs in Nrf2 signaling pathway, WT and Nrf2 knock out (KO) MEF cells were treated with veh or Y-EVs following H₂O₂ exposure. The phosphorylation of JNK, an injury marker, and the gene expression of Nrf2 associated genes were tested in cell lysates. The protein analysis showed Y-EVs treatment reduces the phosphorylation of JNK, an injury marker, following H₂O₂ treatment in WT cells. However, Y-EVs and Veh treatment following H₂O₂ exposure had a similar effect in Nrf2 KO cells (Fig. 8B). Not surprisingly, the levels of Hmox1 and NQO1 were increased while Bach1 and IL6 expression levels were decreased in Y-EVs treated WT MEF cells compared to Veh control. However, there was no significant difference in NQO1, Bach1 or IL6 in Nrf2 KO MEF cells with Y-EVs or Veh treatment (Fig. 8A). Nrf2 insufficiency had a negative impact on the ability of Y-EVs in protecting MEF cells from oxidative stress establishing that Bach1/Nrf2 axis as a critical target of Y-EVs.

DISCUSSION

Plasma EVs contain a heterogeneous group of macro and micro molecules derived from a variety of organismal cells. The cargo of the EVs derived from a normal organism may vary depending on age, sex, genetic background, and the environment. Blood from young animals has been known to have a reparative effect in aging and disease, though the function and identity of the molecular species responsible for the salutary effect remain elusive [33]. Our experiments show that EVs in the blood of young mice have a reparative effect in HI and that the reparative effect observed is due to one or more maturational factors, as the resilience seen in the young mice disappeared in adulthood. Furthermore, the studies demonstrate that the juvenile plasma factors alleviate oxidative stress and improve organ function in the liver. The liver is among the first and major organs affected by the hypoxic insult due hemorrhagic shock [27]. The oxidative injury caused by resuscitation also affects the liver [34]. Though our data suggest that Y-EVs treatment can enhance antioxidant responses and reduce or alleviate oxidative stress following HI, the deficiency of a robust antioxidant response following HI as evidenced by the decreased expression of NQO1, GPX2 and nuclear Nrf2 was surprising. The lack of an increase in the expression of these genes in response to HI-induced oxidative stress is likely a Bach1-mediated effect, a Bach1-dependent impaired Nrf2 inducibility was previously observed with aging [35]. While an increase in the expression of HIF-1 following HI was expected due to HI-induced tissue hypoxia, an increased Bach1 expression after HI was suggestive of Nrf2 dysregulation in HI [36]. Bach1 competes for the Nrf2-MAF binding site on antioxidant

response elements (ARE) on Nrf2 target genes and negatively regulates Nrf2 function [37, 38]. Our results show that the maturation-dependent factors in the Y-EVs enhance antioxidant response by regulating the Bach1-Nrf2 axis.

We also found a significant reduction in the expression of phosphorylated JNK, phosphorylated eIF2 α , as well as NLRP3 in Y-EVs treated animals as compared to vehicle treated animals subjected to HI. JNK/NLRP3 inflammatory signaling plays an important role in mediating hemorrhagic shock-induced tissue injury and JNK is activated by hypoxia, ROS or RNS, and/or various cytokines [39-41]. Moreover, c-Jun/AP-1 activation was associated with an increased inflammatory response, apoptosis, and tissue injury after both H/R and hypoxia. The inhibition of JNK by the protease-resistant JNK inhibitor (D-JNKI-1) before the onset of hemorrhage blunted hepatic damage and local and systemic inflammatory changes after H/R[42]. JNK inhibition after post-hemorrhagic shock also attenuated H/R-induced hepatic injury, neutrophil infiltration, and the production and release of proinflammatory cytokines [43]. The attenuation of the JNK/NLRP3 mediated inflammation following Y-EVs treatment after HI may be attributed to the Nrf2 mediated antioxidant response.

Though it has been recognized for a long time that factors in the blood of young organisms can rejuvenate the old ones, the nature and function of these maturational factors were not fully understood [44-46]. Recent studies using heterochronic parabiosis models further reinforced the hypothesis that juvenile factors can rejuvenate aged systems [47]. A recent study by Rando and colleagues demonstrated a decline of regeneration potential with age that could be reversed through systemic factors in the young [19]. Another study using heterochronic parabiosis showed that old blood has the potential to reduce mitochondrial content and the levels of enzymes involved in oxidative phosphorylation suggesting that age-associated changes in mitochondrial function is influenced by circulating factors [48]. It will be interesting to know whether the EVs isolated from aged mice could aggravate outcome following HI in young mice, as well as their effect on mitochondrial function. Nevertheless, emerging studies indicate an important role for biological fluid-derived EVs including exosomes in cell-cell communications and repair [49-51]. Paracrine signaling as well as distant signaling by soluble factors from stem cells are being increasingly recognized as relevant to disease treatment [52-54]. An increased tissue ATP level, declined oxidative stress and reduced infarct size were observed, in another study, when a single intravenous dose (4 mg/Kg) of stem cell-derived exosomes was given prior to myocardial I/R injury [55].

An empirical analysis of the cargo of Y-EVs to determine the maturational factor is challenging due to the heterogeneous nature of the constituent molecular species. Nevertheless, such unknown systemic factors are postulated to mediate effects on multi-organ function and survival in individuals exposed to insults, and these effects are age and maturational dependent [56-58]

The identification of endogenous juvenile protective factors that demonstrate a salutary effect on aging may not only mitigate the influence of aging on the injury, but may also enable injury resolution and will open a new dimension in the treatment of injuries such as that due to severe blood loss. There is also a need, albeit challenging, to further define the mechanistic underpinnings that confer a protective effect in hemorrhagic shock with respect to maturation and aging including their participation in organ crosstalk and long-distance information sharing. Our finding of the resilience of youthful organisms in response to injury, the salutary effect of plasma-derived EVs from the young in altering outcomes following hemorrhagic shock, and their ability to modulate antioxidant response in the aged animal have profound implications not only for the treatment of low flow conditions, but also for the understanding of the biology of aging.

Acknowledgements

The work was partly supported by NIH grants R01 GM122059 (RPR), R56 AG073338 (RPR) and R01 NS101967 (BT). Authors acknowledge the support of Ms. Marie Warren in conducting some of the mitochondrial respiration and mitochondrial potential measurement studies.

Competing Interests

Authors do not have any competing interests.

Supplementary Materials

The Supplementary data can be found online at: www.aginganddisease.org/EN/10.14336/AD.2021.0830.

References

[1] Burns E, Kakara R (2018). Deaths from falls among persons aged ≥ 65 years—United States, 2007–2016. *Morbidity and Mortality Weekly Report*, 67:509.

[2] Vanzant EL, Hilton RE, Lopez CM, Zhang J, Ungaro RF, Gentile LF, et al. (2015). Advanced age is associated with worsened outcomes and a unique genomic response in severely injured patients with hemorrhagic shock. *Critical care*, 19:1-15.

[3] Poulouse N, Raju R (2014). Aging and injury:

alterations in cellular energetics and organ function. *Aging and disease*, 5:101.

[4] Ham III PB, Raju R (2017). Mitochondrial function in hypoxic ischemic injury and influence of aging. *Progress in neurobiology*, 157:92-116.

[5] Jian B, Yang S, Chen D, Zou L, Chatham JC, Chaudry I, et al. (2011). Aging influences cardiac mitochondrial gene expression and cardiovascular function following hemorrhage injury. *Molecular medicine*, 17:542-549.

[6] Klingbeil LR, Kim P, Piraino G, O'Connor M, Hake PW, Wolfe V, et al. (2017). Age-Dependent Changes in AMPK Metabolic Pathways in the Lung in a Mouse Model of Hemorrhagic Shock. *Am J Respir Cell Mol Biol*, 56:585-596.

[7] Jian B, Yang S, Chen D, Chaudry I, Raju R (2011). Influence of aging and hemorrhage injury on Sirt1 expression: possible role of myc-Sirt1 regulation in mitochondrial function. *Biochim Biophys Acta*, 1812:1446-1451.

[8] Chu X, Wen J, Raju RP (2020). Rapid senescence-like response after acute injury. *Aging Cell*, 19:e13201.

[9] Gutierrez G, Reines H, Wulf-Gutierrez ME (2004). Clinical review: hemorrhagic shock. *Critical care*, 8:1-9.

[10] Powers KA, Szászi K, Khadaroo RG, Tawadros PS, Marshall JC, Kapus A, et al. (2006). Oxidative stress generated by hemorrhagic shock recruits Toll-like receptor 4 to the plasma membrane in macrophages. *The Journal of experimental medicine*, 203:1951-1961.

[11] Itoh K, Chiba T, Takahashi S, Ishii T, Igarashi K, Katoh Y, et al. (1997). An Nrf2/small Maf heterodimer mediates the induction of phase II detoxifying enzyme genes through antioxidant response elements. *Biochemical and biophysical research communications*, 236:313-322.

[12] Niture SK, Khatri R, Jaiswal AK (2014). Regulation of Nrf2—an update. *Free Radical Biology and Medicine*, 66:36-44.

[13] Kensler TW, Wakabayashi N, Biswal S (2007). Cell survival responses to environmental stresses via the Keap1-Nrf2-ARE pathway. *Annu. Rev. Pharmacol. Toxicol.*, 47:89-116.

[14] Conboy MJ, Conboy IM, Rando TA (2013). Heterochronic parabiosis: historical perspective and methodological considerations for studies of aging and longevity. *Aging Cell*, 12:525-530.

[15] Yousefzadeh MJ, Wilkinson JE, Hughes B, Gadela N, Ladiges WC, Vo N, et al. (2020). Heterochronic parabiosis regulates the extent of cellular senescence in multiple tissues. *Geroscience*, 42:951-961.

[16] Scudellari M (2015). Ageing research: Blood to blood. *Nature*, 517:426-429.

[17] Pan M, Wang P, Zheng C, Zhang H, Lin S, Shao B, et al. (2017). Aging Systemic Milieu Impairs Outcome after Ischemic Stroke in Rats. *Aging Dis*, 8:519-530.

[18] Loffredo FS, Steinhauser ML, Jay SM, Gannon J, Pancoast JR, Yalamanchi P, et al. (2013). Growth differentiation factor 11 is a circulating factor that reverses age-related cardiac hypertrophy. *Cell*, 153:828-839.

- [19] Conboy IM, Conboy MJ, Wagers AJ, Girma ER, Weissman IL, Rando TA (2005). Rejuvenation of aged progenitor cells by exposure to a young systemic environment. *Nature*, 433:760-764.
- [20] Shetty AK, Hattiangady B (2007). Concise review: prospects of stem cell therapy for temporal lobe epilepsy. *Stem Cells*, 25:2396-2407.
- [21] Potter DR, Miyazawa BY, Gibb SL, Deng X, Togaratti PP, Croze RH, et al. (2018). Mesenchymal stem cell-derived extracellular vesicles attenuate pulmonary vascular permeability and lung injury induced by hemorrhagic shock and trauma. *J Trauma Acute Care Surg*, 84:245-256.
- [22] Biressi S, Filareto A, Rando TA (2020). Stem cell therapy for muscular dystrophies. *J Clin Invest*, 130:5652-5664.
- [23] Moller A, Lobb RJ (2020). The evolving translational potential of small extracellular vesicles in cancer. *Nat Rev Cancer*, 20:697-709.
- [24] Kalluri R, LeBleu VS (2020). The biology, function, and biomedical applications of exosomes. *Science*, 367.
- [25] Subramani K, Chu X, Warren M, Lee M, Lu S, Singh N, et al. (2019). Deficiency of metabolite sensing receptor HCA2 impairs the salutary effect of niacin in hemorrhagic shock. *Biochimica et Biophysica Acta (BBA)-Molecular Basis of Disease*, 1865:688-695.
- [26] Kolhe R, Hunter M, Liu S, Jadeja RN, Pundkar C, Mondal AK, et al. (2017). Gender-specific differential expression of exosomal miRNA in synovial fluid of patients with osteoarthritis. *Sci Rep*, 7:2029.
- [27] Karmanioliou, II, Theodoraki KA, Orfanos NF, Kostopanagiotou GG, Smyrniotis VE, Mylonas AI, et al. (2013). Resuscitation after hemorrhagic shock: the effect on the liver--a review of experimental data. *J Anesth*, 27:447-460.
- [28] Sims CA, Guan Y, Mukherjee S, Singh K, Botolin P, Davila Jr A, et al. (2018). Nicotinamide mononucleotide preserves mitochondrial function and increases survival in hemorrhagic shock. *JCI insight*, 3.
- [29] Warren M, Subramani K, Schwartz R, Raju R (2017). Mitochondrial dysfunction in rat splenocytes following hemorrhagic shock. *Biochimica et Biophysica Acta (BBA)-Molecular Basis of Disease*, 1863:2526-2533.
- [30] Subramani K, Lu S, Warren M, Chu X, Toque HA, Caldwell RW, et al. (2017). Mitochondrial targeting by dichloroacetate improves outcome following hemorrhagic shock. *Scientific reports*, 7:1-13.
- [31] Lerner N, Chen I, Schreiber-Avissar S, Beit-Yannai E (2020). Extracellular Vesicles Mediate Anti-Oxidative Response-In Vitro Study in the Ocular Drainage System. *Int J Mol Sci*, 21.
- [32] Yarana C, St Clair DK (2017). Chemotherapy-Induced Tissue Injury: An Insight into the Role of Extracellular Vesicles-Mediated Oxidative Stress Responses. *Antioxidants (Basel)*, 6.
- [33] Castellano JM (2019). Blood-Based Therapies to Combat Aging. *Gerontology*, 65:84-89.
- [34] Douzinas EE, Livaditi O, Tasoulis M-K, Prigouris P, Bakos D, Goutas N, et al. (2012). Nitrosative and oxidative stresses contribute to post-ischemic liver injury following severe hemorrhagic shock: the role of hypoxemic resuscitation. *PLoS One*, 7:e32968.
- [35] Zhou L, Zhang H, Davies KJA, Forman HJ (2018). Aging-related decline in the induction of Nrf2-regulated antioxidant genes in human bronchial epithelial cells. *Redox Biol*, 14:35-40.
- [36] Jian B, Wang D, Chen D, Voss J, Chaudry I, Raju R (2010). Hypoxia-induced alteration of mitochondrial genes in cardiomyocytes: role of Bnip3 and Pdk1. *Shock*, 34:169-175.
- [37] Dhakshinamoorthy S, Jain AK, Bloom DA, Jaiswal AK (2005). Bach1 competes with Nrf2 leading to negative regulation of the antioxidant response element (ARE)-mediated NAD(P)H:quinone oxidoreductase 1 gene expression and induction in response to antioxidants. *J Biol Chem*, 280:16891-16900.
- [38] Sun J, Hoshino H, Takaku K, Nakajima O, Muto A, Suzuki H, et al. (2002). Hemoprotein Bach1 regulates enhancer availability of heme oxygenase-1 gene. *EMBO J*, 21:5216-5224.
- [39] Bendinelli P, Piccoletti R, Maroni P, Bernelli-Zazzera A (1996). The MAP kinase cascades are activated during post-ischemic liver reperfusion. *FEBS letters*, 398:193-197.
- [40] Lehnert M, Uehara T, Bradford BU, Lind H, Zhong Z, Brenner DA, et al. (2006). Lipopolysaccharide-binding protein modulates hepatic damage and the inflammatory response after hemorrhagic shock and resuscitation. *American Journal of Physiology-Gastrointestinal and Liver Physiology*, 291:G456-G463.
- [41] Xu P, Wen Z, Shi X, Li Y, Fan L, Xiang M, et al. (2013). Hemorrhagic shock augments Nlrp3 inflammasome activation in the lung through impaired pyrin induction. *The Journal of Immunology*, 190:5247-5255.
- [42] Lehnert M, Relja B, Lee VS-Y, Schwestka B, Henrich D, Czerny C, et al. (2008). A peptide inhibitor of C-jun N-terminal kinase modulates hepatic damage and the inflammatory response after hemorrhagic shock and resuscitation. *Shock*, 30:159-165.
- [43] Relja B, Schwestka B, Lee VS-Y, Henrich D, Czerny C, Borsello T, et al. (2009). Inhibition of c-Jun N-terminal kinase after hemorrhage but before resuscitation mitigates hepatic damage and inflammatory response in male rats. *Shock*, 32:509-516.
- [44] Bruno S, Camussi G (2013). Role of mesenchymal stem cell-derived microvesicles in tissue repair. *Pediatr Nephrol*, 28:2249-2254.
- [45] Herrera MB, Fonsato V, Gatti S, Deregibus MC, Sordi A, Cantarella D, et al. (2010). Human liver stem cell-derived microvesicles accelerate hepatic regeneration in hepatectomized rats. *J Cell Mol Med*, 14:1605-1618.
- [46] Lai RC, Arslan F, Lee MM, Sze NS, Choo A, Chen TS, et al. (2010). Exosome secreted by MSC reduces myocardial ischemia/reperfusion injury. *Stem Cell*

- Res, 4:214-222.
- [47] Zhang W, Qu J, Liu GH, Belmonte JCI (2020). The ageing epigenome and its rejuvenation. *Nat Rev Mol Cell Biol*, 21:137-150.
- [48] Gonzalez-Armenta JL, Li N, Lee RL, Lu B, Molina AJA (2021). Heterochronic Parabiosis: Old Blood Induces Changes in Mitochondrial Structure and Function of Young Mice. *J Gerontol A Biol Sci Med Sci*, 76:434-439.
- [49] Ailawadi S, Wang X, Gu H, Fan GC (2015). Pathologic function and therapeutic potential of exosomes in cardiovascular disease. *Biochim Biophys Acta*, 1852:1-11.
- [50] Long Q, Upadhyia D, Hattiangady B, Kim DK, An SY, Shuai B, et al. (2017). Intranasal MSC-derived A1-exosomes ease inflammation, and prevent abnormal neurogenesis and memory dysfunction after status epilepticus. *Proc Natl Acad Sci U S A*, 114:E3536-E3545.
- [51] Wang X, Gu H, Qin D, Yang L, Huang W, Essandoh K, et al. (2015). Exosomal miR-223 Contributes to Mesenchymal Stem Cell-Elicited Cardioprotection in Polymicrobial Sepsis. *Sci Rep*, 5:13721.
- [52] Ngangan AV, Waring JC, Cooke MT, Mandrycky CJ, McDevitt TC (2014). Soluble factors secreted by differentiating embryonic stem cells stimulate exogenous cell proliferation and migration. *Stem Cell Res Ther*, 5:26.
- [53] Shabbir A, Zisa D, Suzuki G, Lee T (2009). Heart failure therapy mediated by the trophic activities of bone marrow mesenchymal stem cells: a noninvasive therapeutic regimen. *Am J Physiol Heart Circ Physiol*, 296:H1888-1897.
- [54] Singla DK, Singla RD, McDonald DE (2008). Factors released from embryonic stem cells inhibit apoptosis in H9c2 cells through PI3K/Akt but not ERK pathway. *Am J Physiol Heart Circ Physiol*, 295:H907-913.
- [55] Arslan F, Lai RC, Smeets MB, Akeroyd L, Choo A, Aguor EN, et al. (2013). Mesenchymal stem cell-derived exosomes increase ATP levels, decrease oxidative stress and activate PI3K/Akt pathway to enhance myocardial viability and prevent adverse remodeling after myocardial ischemia/reperfusion injury. *Stem Cell Res*, 10:301-312.
- [56] Chang JY, Yi HS, Kim HW, Shong M (2017). Dysregulation of mitophagy in carcinogenesis and tumor progression. *Biochim Biophys Acta*, 1858:633-640.
- [57] Ham PB, 3rd, Raju R (2017). Mitochondrial function in hypoxic ischemic injury and influence of aging. *Prog Neurobiol*, 157:92-116.
- [58] Durieux J, Wolff S, Dillin A (2011). The cell-non-autonomous nature of electron transport chain-mediated longevity. *Cell*, 144:79-91.